

Investigation of Lightning Current Distribution in a Large-Scale Earth-Termination System of Photovoltaic Power Plant

Josef Birkl

DEHN+SÖHNE GmbH + Co. KG.
Neumarkt, Germany
josef.birkl@technik.dehn.de

Eduard Shulzhenko

Group for Lightning and Overvoltage Protection
Technische Universität Ilmenau, Germany
eduard.shulzhenko@tu-ilmenau.de

Abstract— The transient performance of large grounding grids subjected to lightning current impulses is studied in case of photovoltaic (PV) power plant. In this paper various numerical models have been developed which considers different parameters both geometry of grounding mesh system and soil. The maximum transient ground potential rise or GPR and frequency dependent impedance are analyzed in frequency and in transient domains.

Simulation are based on Maxwell equations and Sommerfeld integrals used in XGSLab software package for grounding system analysis. Also, a prospective overvoltage between point of strike and a cabinet at a distance of 300 m is analyzed. A significant reduction of transient ground potential rise is possible only in cases when mesh sizes or separation between conductors are significantly smaller than estimated effective area during lightning performance. For different soil parameters an effective area was estimated in case of first positive lightning current. Also the possibility of reduction of maximal transient GPR as well as reduction of overvoltages between different parts of grounding grid with adjusting of span between conductors is investigated.

Keywords—Photovoltaic (PV) power plant; transient ground potential rise (GPR); earth-termination system; lightning impulse current; numerical model

I. INTRODUCTION

Grounding square grids are an effective solution for earth-termination systems (ETS) of substations and large-scale PV plants. It is desired that these systems provide near zero impedance which ensures the even distribution of conductor potentials. This will provide a safe environment for human and equipment from dangerous potential rises.

During lightning current discharges, the impedance of ETS to earth is becoming larger than the value obtained during low-frequency regimes. It is because of two phenomena: soil ionization and inductance of the ETS. It leads to highly uneven distribution of potentials during transient period. This will lead to high voltages between different parts of grounded

structures (e.g. cabinet) generating hazardous conditions for the human beings and the equipment.

The behavior of ETS at low frequencies is well known and described [1]. However, analysis of ETS subjected to lightning impulse current is more complicated. Most of the previous work on this subject relates to simple grounding arrangements or the introduced numerical models have numerous simplifications or based on quasi-static approximation. The validity of such numerical approaches may be limited to some upper frequency, which depends of ETS and electrical characteristics of the soil. Also, an electromagnetic approach using finite element method (FEM) is ineligible for large-scale ETS because of model complexity and calculation time.

The initial part of lightning impulse current is discharged into the earth through a relative small area of the ETS around of the feed point. This area enlarges over the time as the impulse current spreads through ETS and at the end it encompasses the whole ETS [2]. In this case two stages can be distinguished: the initial surge period (before the impulse current reaches the end of the ETS) and the late stationary period (the impulse current reaching the end of the ETS). The initial surge stage is characterized by uneven distribution of conductor potentials (the potential is reaching maximum value). The second stage is characterized by discharging of current into earth through the whole ETS with even distribution of potentials that is typical for low-frequency regimes. The first period is more dangerous because of the large current and small discharging area which causes highly uneven potential distributions. This could cause danger to people and equipment [3].

To be able to describe the behaviour of ETS under lightning surge conditions, both the impulse impedance Z and impulse coefficient A are used [4]:

$$Z = \frac{V_m}{I_m}, \quad A = \frac{Z}{R_{LF}} \quad (1)$$

where V_m and I_m are maximum values of voltage and current at the feed point, respectively; R_{LF} – ETS resistance at the low or power frequency. The impulse coefficient A allows to compare the grounding performance under surge / lightning conditions with the performance at the power frequency.

The purpose of the study of this paper was first to investigate the influence of different parameters both geometry of ETS (span between grounding conductors S as well as square grid-side length a) and soil during lightning current discharging into earth. Second, the obtained maximum transient ground potential rise or TGPR (voltage between the ETS and the remote neutral earth) and frequency dependent impedance are analyzed in frequency domain (FD) with corresponding equivalent frequency f_{eq} for an impulse current discussed below and the results are compared with those obtained in time domain (TD). Also an effect of reduction of maximal TGPR as well as reduction of overvoltages between different parts of ETS with adjusting of span between grounding conductors S is investigated.

II. NUMERICAL MODEL

A. Numerical Approach

The XGSLab (over and underground system laboratory) software package for grounding system analysis was used for designing of numerical models presented in this paper. Recently, the software package is capable to do the calculation in the TD due to the Fourier transform. The designed numerical models focused on the inductive effects and without considering of an effect of the soil ionization since it is likely to be small and can be neglected for grounding grids [4].

B. Impulse Current

The inductance has a major influence on maximum TGPR during fast front current pulses. Therefore, the representation of realistic lightning impulse current waveform is essential. It was reproduced by means of Heidler's function [5], [6]:

$$i_L(t) = \frac{\hat{I}}{\eta} \left(\frac{t}{\tau_1} \right)^n \frac{1}{1 + \left(\frac{t}{\tau_1} \right)^n} \cdot e^{-\frac{t}{\tau_2}} \quad (2)$$

where \hat{I} is peak value of the lightning current, η is correction factor for the current peak, $n = 10$ – constant, τ_1 and τ_2 are rising and falling time constants, respectively.

This current function is very frequently used in lightning research, e.g. it is proposed by CIGRE, Working Group 33.01. In several standards, as in IEC 62305-1 [7], the lightning currents are based on this function. Sometimes the sum of two Heidler functions is used to approximate the desired current wave shape [8], [9], [10]. This modified function is essential for any numerical simulation since it allows to reduce the time offset (before an essential current starts to flow). The approach with the sum of two Heidler functions is commonly used in the literature for investigation of grounding grid dynamic behaviour (e.g. [11]), because it represents better the realistic

lightning current waveshape with observed concave rising portion of recorded lightning current impulses [12].

The initial investigation was performed for first positive impulse current wave shape 10/350 μ s, 100 kA according to lightning protection level III and IV [7] with simple Heidler function (2).

Two types of homogeneous soil are considered: 1) “wet soil” with resistivity $\rho_s = 100 \Omega \cdot m$ and relative permittivity $\epsilon = 36$ and 2) “dry soil” with $\rho_s = 1000 \Omega \cdot m$ and $\epsilon = 9$ [14]. Location of the feed point is chosen at the corner since the maximal TGPR in this case is much higher than it reaches at the centre [11], [13]. The computations are made for the depth of the grid $d = 0.5$ m in uniform soil.

The considered side length of the square ground grid for ETS $a = 1000$ m (Fig. 1) and it is composed of square meshes with the spacing between conductors S which varies in a range from 5 m to 500 m.

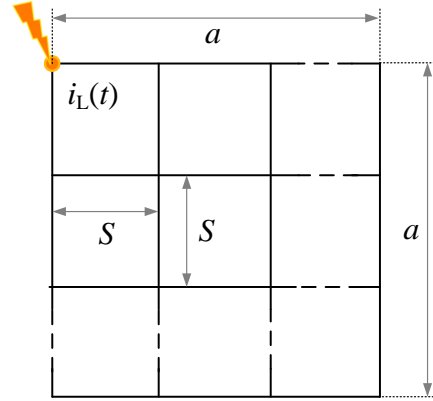


Fig. 1. Square ground grid of PV plant

C. Validation

For validation of numerical approach used in this paper, the experimentally determined grounding grid impulse characteristics from [15] are used. The considered here square ground grid has its grid-side length $a = 10$ m and conductor spacing $S = 5$ m, buried at the depth of $d = 0.6$ m, radius of the copper conductors is 7 mm. Three configurations of grounding grid were observed in the paper and for validation purpose the “Configuration II” has been chosen (Fig. 2). The grounding system consists of two soil layers with the resistivity $\rho_1 = 50 \Omega \cdot m$ and $\rho_2 = 20 \Omega \cdot m$, respectively. Two different impulse current wave shapes were chosen from the paper [15] for our observation, which were achieved with adjusting a pre-resistor “ R ” in introduced test set-up: with $R = 6 \Omega$ the impulse current wave shape was 6.9/77.8 μ s with its peak current $\hat{I} = 10$ A (Fig. 3 a)); with $R = 15 \Omega$ the impulse current wave shape was 14/97.7 μ s with $\hat{I} = 8.5$ A (Fig. 3 b)).

First these two current wave shapes were fitted with double-exponential function for finding their parameters (rising and falling time constants τ_1 and τ_2 , their correction factors for peak value η), which are given in Fig. 3 as well.

Then, the impulse currents were injected at the corner of the grid (Fig. 2, point A). Finally, the voltages at the points A and B were compared with our computation model. Fig. 3 shows a comparison between measured voltages from the paper [15] and our computation results. A visual comparison shows a good agreement of measured and calculated voltages. Some small reflection on the measured impulse voltages in the front could be seen. Those are the reflections caused by a slight impedance mismatching between the coaxial feeding cable and the tested grounding grid configuration connected thereto.

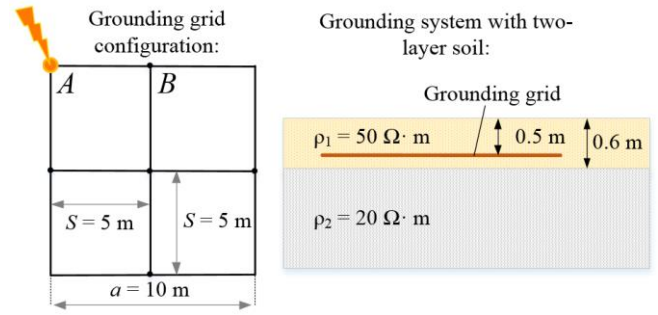


Fig. 2. The analyzed grounding grid configuration

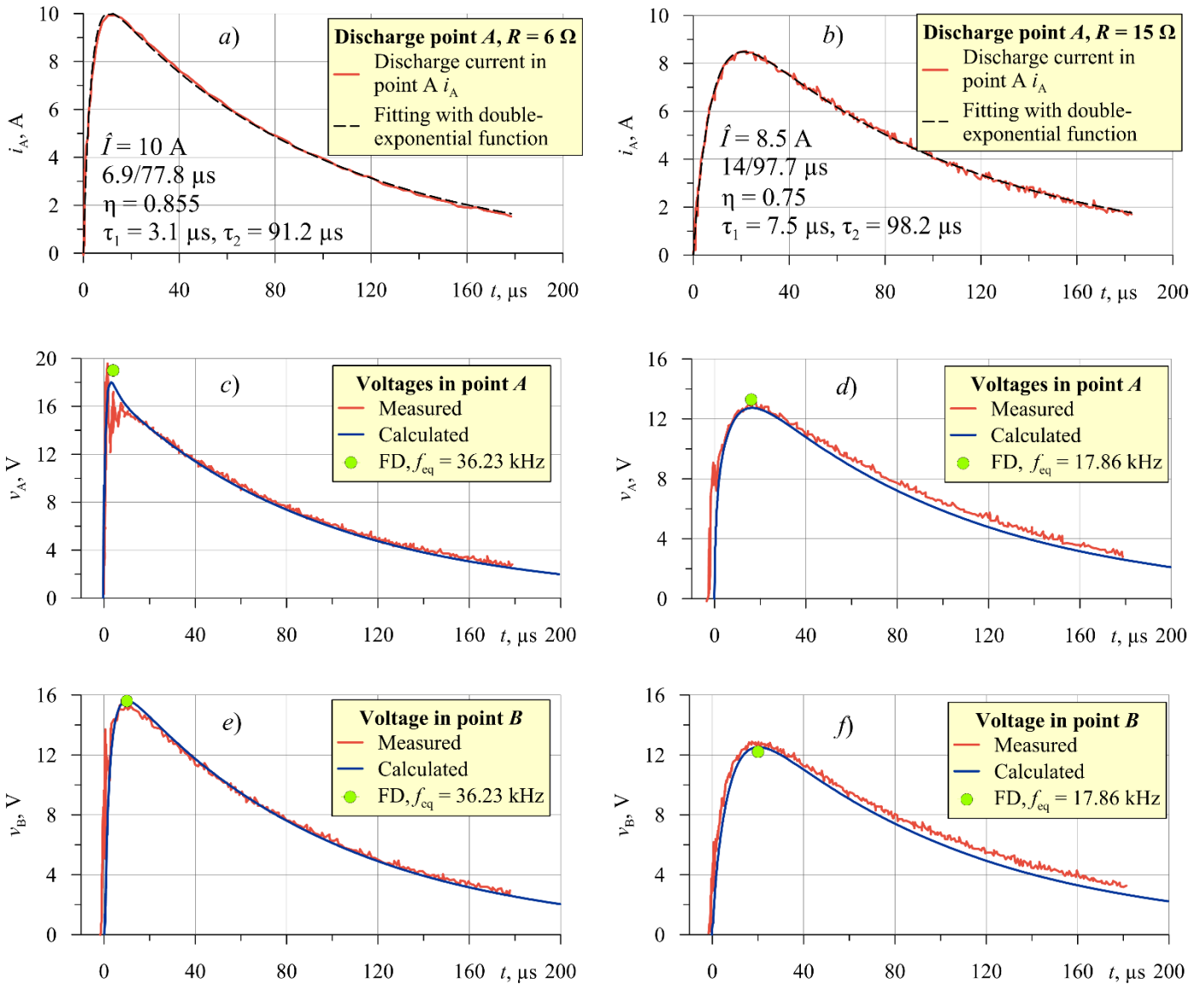


Fig. 3. Comparison between measurements from [15] and numerical approach

Using formulas (1) for the case *a*), the measured value of impulse impedance is $Z = 18 \text{ V}/10 \text{ A} = 1.8 \Omega$ and impulse coefficient is $A = 1.8 \Omega/1.73 \Omega \approx 1$ – it tells that the grid side *a* (in this case $a = 10 \text{ m}$) was smaller than the side of the impulse effective area.

III. FREQUENCY DOMAIN

The numerical model based on FD could significantly reduce the time calculation and save computer resources. The main purpose of the investigation in FD is to see if such numerical model can be helpful by analyzing of lightning current impact on ETS. For this, an equivalent frequency f_{eq} of impulse current is considered. The value of this frequency can be defined as follows:

$$f_{eq} = \frac{1}{4 \cdot T_1}. \quad (3)$$

In this case, the sine wave with the frequency f_{eq} represents the fast-rising front of impulse current characterized by the front time T_1 . It is essential to reproduce the initial surge period in FD, since the maximal transient GPR occurs during this stage. In case of first positive impulse $10/350 \mu\text{s}$ this frequency equals $f_{eq} = 25 \text{ kHz}$.

Fig. 4 shows a potential distribution at the surface for two grounding grid configurations, with $S = 40 \text{ m}$ (for “wet” soil case *a*) and for “dry” soil case *b*) and $S = 200 \text{ m}$ (for “wet” soil case *c*) and for “dry” soil case *d*).

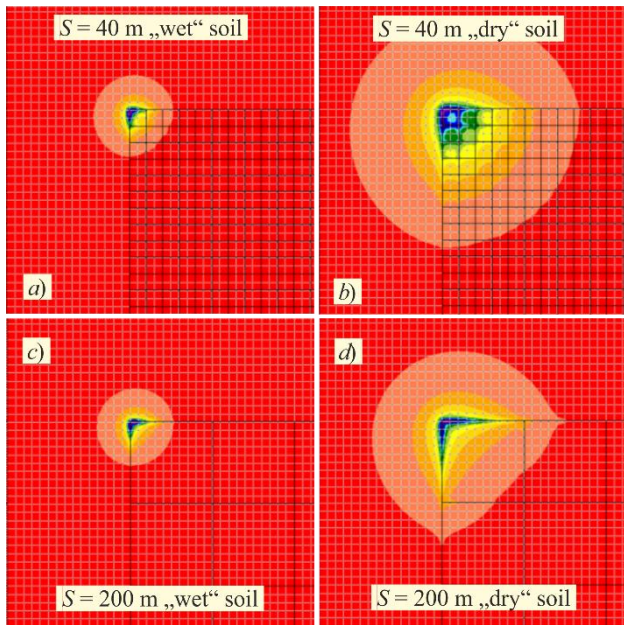


Fig. 4. Potential distribution at the surface

It can be seen that the discharge area (or effective area where the current is discharged into the earth) in “wet” soil (case *a*) and *c*) is smaller than in case with the “dry” soil (case *b*) and *d*). Both configurations of grounding grid show that initial impulse current, which is in this case represented with equivalent frequency f_{eq} , is discharged into the earth through

a relatively small area of grounding system around the feed point.

According to simulation results, at $f_{eq} = 25 \text{ kHz}$ only relative small part of the whole large-scale ETS can be utilized to leak out the current during the initial surge period of impulse discharge. Therefore, the increasing of ETS size will have no effect on both the maximum TGPR and impulse impedance Z since it has no effect on impulse effective usage area during surge period. The depicted shape of effective area for corner injection is triangular as it described Gupta-Thapar [4].

In Fig. 5 and Fig. 6 the potential distributions alongside the grid conductor at the earth surface \hat{U}_s for different soils and different ETS configurations are shown.

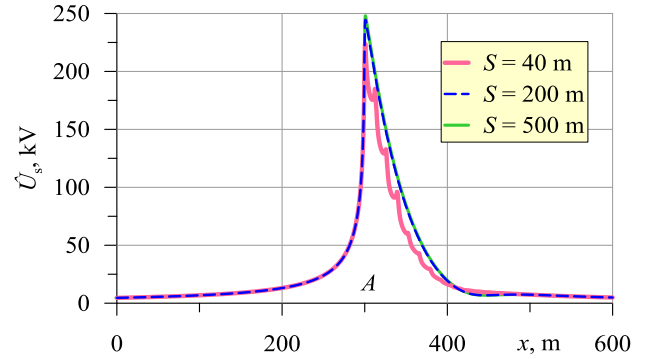


Fig. 5. Potential distribution at the earth surface in case of “wet” soil for different grid configurations

In case of “wet” soil (Fig. 5) the observed range of conductor spacing S from 500 m to 40 m shows almost no effect on reduction of voltage distribution. It implies that the effective area of analyzed grid configurations is less than $40 \times 40 \text{ m}^2$. Later it could be shown during TD simulations. In case of “dry” soil the mentioned reduction can be seen in case when the span between grounding conductors is $S = 40 \text{ m}$ (Fig. 6).

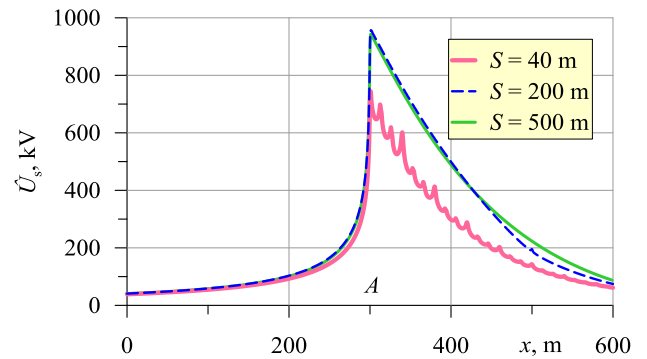


Fig. 6. Potential distribution at the earth surface in case of “dry” soil for different grid configurations

It is clearly, the significant reduction of maximum TGPR is possible with smaller span S between grounding conductors of ETS so that the larger number of conductors within the effective area can be placed. In this case, the more soil can be used to leak impulse current. The numerical model in FD also showed that the effective area in high resistivity soil is larger.

IV. TRANSIENT DOMAIN

For optimization of grounding-grid design, its effective area should be estimated during lightning current performance. This was done during analyzing of transient performance of ETS with inner mesh sizes ranging from $3 \times 3 \text{ m}^2$ to $500 \times 500 \text{ m}^2$ and compared with several equations proposed by previous researches.

A. Dynamic Behaviour of ETS

The characteristic of the inductive behaviour that causes the maximal TGPR in the first moments of the lightning strike is demonstrated in Fig. 7. The considered grid (with its square grid-side length $a = 1000 \text{ m}$ and span between grounding conductors $S = 100 \text{ m}$) is hit by a lightning impulse current $10/350 \mu\text{s}$ at the corner. Two different soils, referred as “dry” and “wet” soil (see chapter 2) are considered. The computed values are normalized to the impulse peak current value \hat{I} . During the initial surge stage the dynamic behaviour of ETS is dominantly inductive and larger than $i_L \cdot R_{LF}$ – the purely resistive dynamic performance of the ETS during low-frequency (dotted lines in Fig. 7).

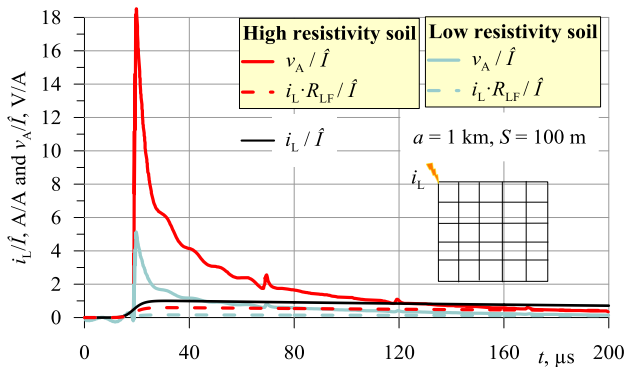


Fig. 7. Dynamic behaviour of the ETS in case of corner strike for two soils

The extent of the impairment of the ETS performance is larger in high resistivity soil (red line v_A / \hat{I} in Fig. 7). The peak values in Fig. 7 deliver impulse impedance Z (1): for low resistivity soil $Z = 5.2 \Omega$ (the computed low-frequency resistance was $R_{LF} = 0.12 \Omega$) and for high resistivity soil $Z = 18.5 \Omega$ ($R_{LF} = 0.51 \Omega$). Therefore, impulse coefficient (1) $A = 43$ for “wet” soil and $A = 36$ for “dry” soil. These values of A give an idea of the maximal rates of impairment of the ETS performance in comparison to the low-frequency performance during the first positive stroke.

B. Impulse Effective Area

Effective area is an important criterion for improving ETS performance during lightning current. The inductive effect obstructs the lightning current during the initial surge stage to flow toward the distant end of the ETS. Therefore only part of the ETS can be utilized to leak out the impulse current. This limiting area of ETS around the feed point controls the impulse impedance and defined as an impulse effective area. The practical meaning of this area is that the employing denser mesh within this area will consequently reduce the ETS impulse impedance. For this reason, the side-length a_e is

considered instead of radius of effective area. In the literature the impulse effective area is usually defined as the area of a grid beyond which the decrement of transient impedance at the injection point has decreased to a value within 3 % of the final maximum transient impedance of the grid [4] [16].

Table 1 shows calculated side-length values a_e of effective area with different numerical approaches for different front times T_1 for “wet” ($\rho_s = 100 \Omega \cdot \text{m}$) and “dry” ($\rho_s = 1000 \Omega \cdot \text{m}$) soils. First two approaches (Gupta and Thapar [4], Zeng [16] with consideration of soil ionization) are based on circuit method and the third approaches proposed by Grcev is based on electromagnetic method [11].

TABLE I. EVALUATED IMPULSE EFFECTIVE RADIUS FOR DIFFERENT SOILS IN CASE OF TD ($T_1 = 10 \mu\text{s}$, FOR CORNER-FED GRID)

$\rho_s, \Omega \cdot \text{m}$	Impulse effective area side-length a_e, m			
	Gupta		Zeng	Grcev
	$S = 5 \text{ m}$	$S = 20 \text{ m}$		
100	27	6	5.4	23
1000	84	18	14	293

All methods seems give different results. In [17] the authors found out for their grid that Gupta and Grcev approaches have indantical values. But by higher values of both soil resistivity and front time ($\rho_s = 1000 \Omega \cdot \text{m}$ and $T_1 = 10 \mu\text{s}$) these two approaches delivers diverent values.

In case of high resistivity soil the effective area is larger (Table 1 and also Fig. 5 and Fig. 6). To be able to reduce maximal TGPR, the larger number of conductors within this defined effective area need to be considered. In the next chapter the obtained values will be compared with the results from introduced numerical model.

C. Comparison between FD and TD / Influence of conductor spacing on maximal TGPR

For comparison, the investigated Configuration II above was taken (Fig. 3). The simulation results in FD were also added to the diagrams (green points). The simulations were performed with an equivalent frequencies f_{eq} . In case of first impulse current $6.9/77.8 \mu\text{s}$ this equivalent frequency according to (3) equals 36.23 kHz , in case of the second impulse current $14/97.7 \mu\text{s}$ – 17.86 kHz . The diagram in Fig. 3 shows perfect match between maximal TGPR value and maximal value of the voltages at different nodes (points A and B) obtained in FD. Therefore, the FD with corresponding f_{eq} can be used for accurate estimation of maximal TGPR during impulse current, also in case of multilayer soil.

In this regard, the influence of conductor spacing S on maximal TGPR is investigated with help of FD for square grid-side length $a = 1000 \text{ m}$ (Fig. 8). Again, two cases are considered with different soil conductivities discussed above.

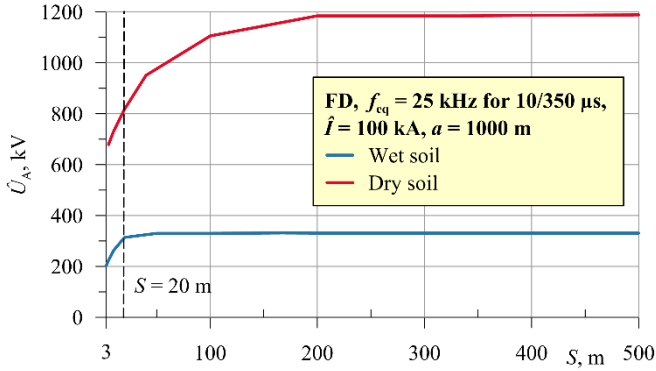


Fig. 8. Influence of span between grounding conductors of ETS on GPR

First, the maximal evaluated surge potential values at the feed point \hat{U}_A (at the corner of the grid) in case of “dry” soil are higher than those obtained for “wet” soil. Second, the values of maximal TGPR remain constant if S is larger than the side-length of an impulse effective area a_e . Third, by achieving S the side-length of effective area a_e the surge potential (or surge impedance) starts decreasing and in case of “dry” soil this decreasing takes place earlier. By comparing this results with the results obtained in the Table 1, the approach from Grcev seems to have a good agreement. According to the simulation results, in case of “wet” soil (Fig. 8) the effective area is approached by $S \approx 20$ m and in case of “dry” soil by $S \approx 200$ m. The predicted values of side-length of effective area were 23 m and 293 m correspondingly which are the closest values to our simulation results. In this regard, the Grcev approach could be used in the wide range of values of both time front and soil resistivity for evaluation of size of effective area.

D. Prospective overvoltage between point of strike and a cabinet at 300 m distance

Fig. 9 illustrates the dependence of the differential potential \hat{U}_{300} between the feed point at the corner and the distant point at the span at the distance of 300 m (for example where a cabinet can be located).

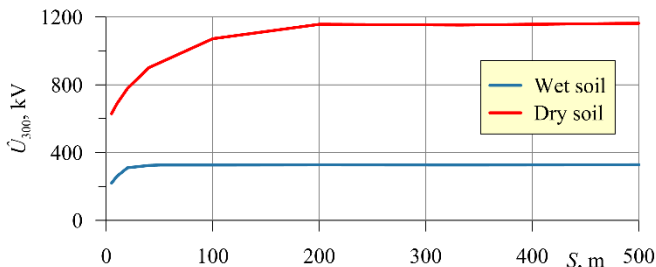


Fig. 9. Influence of span between grounding conductors of ETS on GPR

There is no significant difference with voltage distribution demonstrated in Fig. 8 for the feeding point. The reason is that the voltage drops took places in the range of effective area (which is less than 300 m) and at the distance of 300 m the voltage at the grid span reaches 2 – 3 kV in the case of the “wet” soil and about 30 kV in the case of the “dry” soil.

Only by reaching S the values of impulse effective area side length (e.g. $S < 23$ m = a_e in case of low resistivity soil, Table 1), the maximal TGPR starts decreasing, which in turn can reduce the potential difference ΔU_{300} considerably. Thus, the impulse effective area during designing of ETS should be considered for controlling / reduction of overvoltage between different points of ETS which can endanger electrical and electronic equipment or generate hazardous conditions for human beings.

V. CONCLUSION

A numerical model is presented for large-scale earth-termination system (ETS) designed in XGSLab software, which is based on Maxwell equations and Sommerfeld integrals.

1. The validation of the numerical approach in case of complicated model with two soil layers showed a good agreement with experimental results. During this validation in time domain (TD) it was shown that the maximal TGPR could be successfully reproduced in frequency domain (FD) with equivalent frequency f_{eq} .
2. Further initial investigation was performed on a large-scale earth-termination system (ETS) for first positive lightning current 10/350 μ s, 100 kA. Different parameters of both soil and ETS were considered during simulation.
3. Simulation showed that an impulse current is discharged through a relatively small area of ETS around the feed point during initial surge period. The area around feeding point enlarges in case of soil with higher resistivity. This area is usually called an impulse effective usage area or just an effective area, where the impulse current is actually leaking out to earth during its initial stage. Namely during this initial stage of current an inductive behavior of ETS can be observed (Fig. 7) and where the maximal TGPR occurs. To be able to control TGPR, the ETS design should consider the impulse effective area by selecting an appropriate span between grounding conductors. In this case, increasing of ETS size has no effect on maximal TGPR at all (only for power frequency it is the case).
4. By estimation of effective area side-length during impulse current for the wide range of values of both time front and soil resistivity, the Grcev approach showed a good agreement with the results obtained by presented numerical model and could be also use for large-scale ETS.
5. Estimated values of effective area side-length a_e : for low resistivity soil ($\rho_s = 100 \Omega \cdot m$) $a_e \approx 20$ m and for high resistivity soil ($\rho_s = 1000 \Omega \cdot m$) $a_e \approx 290$ m. It means that for significant reduction of TGPR, the inner mesh of ETS should be much smaller than 20×20 m² for considered low resistivity soil and smaller than 290×290 m² for considered high resistivity soil.
6. The prospective overvoltage between point of strike and a cabinet at suggested 300 m distance (Fig. 9) have almost the same behavior as the voltage measured at the strike point directly against distant potential (Fig. 8). The reason for that is that the impulse effective area was much smaller for considered cases as the considered distance of 300 m. By

considering of effective area size, the overvoltage between different points of ETS can be reduced significantly. This can be achieved by selecting appropriate span between conductors.

The presented information in this paper can be helpful for design or upgrade existed ETS for reliable protection against lightning. Enlarging the area of the grounding grid is an effective measure to reduce the power-frequency grounding resistance and limit the GPR at this frequency. However, in order to reduce the impulse grounding resistance as well as overvoltage between different parts of ETS) generated by the impulse current, enlarging the area of the grounding doesn't have any effect. But increasing the number of the conductors near the feed points will be an effective measure.

REFERENCES

- [1] ANSI/IEEE Std. 80-2000: Guide for Safety in AC Substation Grounding, New York, 2000.
- [2] L. D. Grcev, "Computer analysis of transient voltages in large grounding systems," IEEE Transactions on power delivery, vol. 11, No. 2, pp. 815–823, 1996.
- [3] CIGRÉ guide on electromagnetic compatibility in electric power plants and substations, Tech. Brochure 124. Paris, France, Dec. 1997.
- [4] B. R. Gupta and B. Thapar, "Impulse impedance of grounding grids," IEEE Trans. Power App. Syst., vol. PAS-99, No. 6, pp. 2357–2362, Nov. 1980.
- [5] F. Heidler, "Analytische Blitzstromfunktion zur LEMP-Berechnung," Proc. of the 18th International Conference on Lightning Protection, Munich, 1985, pp. 63–66.
- [6] F. Heidler and J. Cvetić, „A class of analytical functions to study the lightning effects associated with the current front.“ European transactions on electrical power, vol. 12, No. 2, pp. 141–150, 2002.
- [7] IEC 62305-1:2010 Protection against lightning – Part 1: General principles.
- [8] V. Rakov, "Lightning: Physics and Effects," Cambridge: Cambridge University Press, 2010.
- [9] F. Rachidi et al., "Current and electromagnetic field associated with lightning-return strokes to tall towers," IEEE Transactions on Electromagnetic Compatibility, 2001, vol. 43, No. 3, pp. 356–367.
- [10] V. Cooray Ed. "Lightning protection," Institution of Engineering and Technology, London, 2010.
- [11] L. Grcev, "Lightning Surge Efficiency of Grounding Grids," IEEE Transactions on Power Delivery, vol. 26, No. 3, pp. 1692–1699, Jul. 2011.
- [12] K. Berger, R. B. Anderson, and H. Kroninger, "Parameters of lightning flashes," Electra, No. 41, pp. 23–37, 1975.
- [13] L. D. Grcev and M. Heimbach, "Frequency dependent and transient characteristics of substation grounding systems," IEEE Transactions on Power Delivery, vol. 12, No. 1, pp. 172–178, 1997.
- [14] A.P. Meliopoulos and M.G. Moharam, "Transient Analysis of Grounding Systems" IEEE Transactions on Power Apparatus and Systems, vol. 102, pp. 389–399, Feb. 1983.
- [15] Z. Stojkovic, M. S. Savic, J. M. Nahman, D. Salamon, and B. Bukorovic, „Sensitivity analysis of experimentally determined grounding grid impulse characteristics,“ IEEE Transactions on Power Delivery, vol. 13, No. 4, pp. 1136–1142, 1998.
- [16] Rong Zeng, Xuehai Gong, Jinliang He, Bo Zhang, und Yanqing Gao, „Lightning Impulse Performances of Grounding Grids for Substations Considering Soil Ionization,“ IEEE Transactions on Power Delivery, vol. 23, No. 2, pp. 667–675, Apr. 2008.
- [17] F. Hanaffi F., W.H. Siew, I. Timoshkin, Hailiang LU, Yu Wang, Lei Lan, Xishan Wen, "Evaluation of grounding grid's effective area," Proc. of the 32 International Conference on Lightning Protection (ICLP), pp. 402–406, Shanghai, China, 2014.